

Computing Deform Closure Grasps^{*}

K. “Gopal” Gopalakrishnan¹ and Ken Goldberg²

¹ IEOR Department, U.C. Berkeley, USA

² IEOR and EECS Departments, U.C. Berkeley, USA

Abstract. In prior work, we extended the well-known form closure grasp framework for rigid parts to a class of deformable parts, modeled as frictionless polygons with a finite element mesh and given stiffness matrix. We define the *D-space* (deformation-space) of a part as the C-space of all its mesh nodes and *deform closure* in terms of the work needed to release the part from a set of finger contacts.

In the present paper, we define a measure of grasp quality for two-point deform-closure grasps. This metric is based on balancing the potential energy needed to release the part against the potential energy that would result in plastic deformation. Given two jaw contacts at the perimeter nodes, we give a numerical algorithm to determine the optimal jaw separation based on this metric. For a part with n mesh nodes and p perimeter nodes, the algorithm computes an approximation to the optimal separation in time $O(n^3 p^2 + (p^2/\epsilon) \log p)$.

1 Introduction

There is a substantial body of research on robotic holding (grasping and fixturing) of rigid objects. Our work is inspired by Rimon and Burdick on rigid body immobility [Rimon96] and by Rimon and Blake [Rimon99] on caging grasps for rigid bodies. We adopt their notation wherever possible.

In [Gopalakrishnan04], we proposed a new model for grasping deformable parts that combines ideas from C-space, FEM meshing, and cage grasping. We define D-space based on the degrees of freedom of mesh nodes and "deform closure" based on local minima in elastic potential energy.

In the present paper, we define a measure of grasp quality for two-point deform-closure grasps. This metric is based on balancing the potential energy needed to release the part against the potential energy that would cause plastic deformation. Given two jaw contacts at the perimeter nodes, we give a numerical algorithm to determine the optimal jaw separation based on this metric.

In our model, the part perimeter behaves like a planar structure whose perimeter is composed of struts of variable length, with hinges at each vertex. We define the *D-space* (deformation-space) of the part as the C-space of all nodes in its mesh. Given the initial configuration q_0 of the mesh in D-space,

^{*} This work was supported in part by the Ford Motor Company URP 2000-403R and NSF Award DMI-0010069. For more information, please contact goldberg@ieor.berkeley.edu or gopal@ieor.berkeley.edu.

we define D_T as the set of all configurations with the same mesh topology as q_0 . We consider contact with a set of rigid finger bodies $A = \{ A_1, \dots, A_k \}$. Each finger defines a D-obstacle DA_i , the set of mesh configurations that collide with A_i . The free space D_{free} is the set of feasible configurations, the intersection of D_T with the complement of the union of D-obstacles.

Given part E , mesh M , FEM stiffness matrix K , and contact set A , we can determine the potential energy of any point in D_{free} . Given a candidate configuration q_A , we say that the part can be *released* from A by a sequence of external wrenches if the part can escape from q_A . We define U_A as the minimum work that needs to be done by these wrenches to release the part from A . We say that A holds E in *deform closure* if $U_A > 0$.

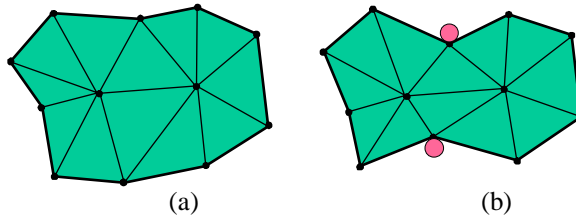


Fig. 1. (a) Deformable part, modeled as a polygon with a finite element mesh and given stiffness matrix. The part perimeter behaves like a planar structure whose perimeter is composed of struts of variable length, with hinges at each vertex (b) The same part held in *deform closure* by two frictionless point contacts.

As intuition behind our algorithm for computing the optimal jaw separation, consider a "contact graph", where each graph vertex corresponds to a pair of mesh nodes. For each vertex, consider a potential energy function based on varying the distance between the underlying mesh nodes. Given two initial mesh nodes where contact occurs, consider a sequence of vertices -- a path -- that leads to an equilibrium grasp configuration. The upper envelope of the potential functions for all vertices on this path corresponds to the maximal potential energy function for the path. Then consider all possible paths, and the lower envelope of all path potential energy functions. The difference between this lower envelope and the potential function at the initial pair of mesh nodes is the minimum work as a function of jaw separation. The potential energy needed to produce plastic deformation is a quadratic function of jaw separation. The lower envelope of the minimum work function and the plastic deformation function yields the objective function, which defines the optimal jaw separation.

This objective function is continuous and piecewise differentiable, but may have an exponential number of pieces. Our algorithm computes the value of the function by uniform sampling, using a sampling interval that is based on stiffness coefficients and a given approximation bound. At each sample point,

we use a dynamic programming algorithm to determine the threshold potential energy and thus the objective function value. The sample point with the maximal value of the objective function provides the approximation to the optimal jaw separation.

2 Related Work

Bicchi and Kumar provide a concise survey of literature on grasping and fixturing in [Bicchi00]. Grasps of rigid bodies can be classified as force or form closure. Form closure (immobility) occurs when any neighboring configuration of the part results in collision with an obstacle. Force-closure occurs if any external wrench can be resisted by applying suitable forces at the contacts [Mason01, Rimon98]. Gripper contacts can be modeled as frictional points, frictionless points or soft contacts [Salisbury82].

The mobility of rigid bodies in contact with frictionless finger bodies was initially studied using first order approximations [Realeaux1876, Somoff1900, Mishra87, Markenscoff90]. The first order theories are based on approximations of part geometry in infinitesimal neighborhoods and part motion of an infinitesimal length. However, these first order approximations of mobility did not always predict immobility correctly.

Rimon and Burdick [Rimon96] give rigorous definitions of first and second order immobility. They express paths of the part in free space using functions $q(t)$ based on scalar parameter t . They consider the distances d_i from the i^{th} C-obstacle surface to $q(t)$. They then consider the first and second order terms in the algebraic expressions of distances as a function of t . The second order terms are needed if first order tests do not show if the distance is increasing or decreasing (the derivative at $t = 0$ is 0). Geometrically speaking, the first order approximation of immobility is equivalent to approximating the trajectory of the part in C-space as a straight line, and the surfaces of the C-obstacles as hyperplanes. Second order immobility is equivalent to approximating the trajectory as an elliptical arc and the C-obstacle surfaces as ellipsoids.

Rimon and Blake [Rimon99] give a method to find caging grasps, configurations of jaws that constrain parts in a bounded region of C-space such that actuating the gripper results in a unique final configuration. They consider the opening parameter of the jaws as a function of the jaws' positions along the perimeter of the part and use stratified Morse theory to find caging grasps by finding limiting cases that occur when the opening parameter is at a saddle point. [Gopalakrishnan02] also uses the distance function to determine immobile grasps of 2D polygonal parts by a pair of vertical cylindrical jaws engaging the part at its concave vertices.

An efficient geometric algorithm to compute all placements of four frictionless point contacts on a polygonal part that ensure form closure is described by van der Stappen et al [vanderStappen99]. Given a set of four

edges, they show how to compute critical contact placements in constant time. The time complexity of their algorithm is bounded by the number of such sets, and runs in an expected time of $O(n^2 \log n)$ for n vertices. Cheong et al [Cheong03] give fast algorithms to find immobilizing grasps of 2D polygonal parts with 2 and 3 contacts. The algorithms find sets of contact wrenches that contain the center of mass. Zhu et al [Zhu03] give a grasp metric for 2D and 3D grasps to quantify how firmly the rigid part is held when resisting external forces. Their metric is faster to compute than similar earlier metrics.

Cheong et al [Cheong02] give upper bounds on the number of point contacts needed to hold a chain of polygons hinged at connecting vertices. They consider the centers of rotation for each polygon such that the hinge vertices have the same linear velocities for the pair of polygons they connect. They place contacts such that no such rotation is possible. Milgram and Trinkle [Milgram02] describe the topology of C-spaces of mechanisms that consist of chains of links connected by rotational joints.

[Ramamurti98] gives an excellent review of finite element methods and speed and memory optimizations for numerical solutions of FEM problems. To solve an FEM problem with n elements exactly, $O(n^3)$ time is required. The numerical approximation makes use of the fact that FEM stiffness matrices are sparse. As a result, there are only $O(n)$ non-zero entries in a matrix with n^2 elements. [Corman90] presents several graph algorithms and data structures. Of particular interest to our algorithm is the proof of correctness and time complexity of the modified Dijkstra's algorithm for sparse graphs implemented with binary heaps. For a graph with n vertices and $O(n)$ edges, the shortest path can be computed in $O(n \log n)$ time.

Recent work on fixturing deformable and sheet-metal parts is based on the work of Menassa and De Vries [Menassa91] where they determine the positions of the primary datum (the datum points needed to locate the part in the correct plane) for 3-2-1 fixturing to minimize deformation. They use a finite element model of the part, and determine fixture locations by optimizing an objective that is a function of the deformations at the nodes. Their work is extended by [Rearick93] and [Cai96].

Gopalakrishnan et al [Gopalakrishnan03] propose *unilateral fixtures*, a new class of fixtures for sheet metal parts with holes, where holding elements lie almost completely on one side of the part, maximizing access for welding, assembly, or inspection. Each primary jaw is cylindrical with a conical groove that provides the equivalent of four point contacts and facilitates part alignment. They present a two-phase algorithm for computing unilateral fixtures where the second phase uses a Finite Element Method (FEM) to compute part deformation and to arrange secondary contacts at part edges and interior surfaces. For a given sheet-metal part, given as a 2D surface embedded in 3D with e edges, n concavities and m mesh nodes, Phase I takes $O(e + n^{4/3} \log^{1/3} n + g \log g)$ time to compute a list of g pairs of primary jaws

ranked by quality. Phase II computes the location of r secondary contacts in $O(g m^3 r)$ time.

Wakamatsu et al [Wakamatsu96] extend the concept of force closure for rigid parts with unbounded applied forces to deformable parts with bounded applied forces. They consider a candidate grasp and external forces within a bound that can deform and displace the part. They assume that the contact normals do not vary as forces are applied, but allow contacts to be broken. They define "bounded force closure" as grasps that can resist any external force within the bound.

Howard and Bekey [Howard97] model deformable parts using a spring-mass model and use a neural network to control a gripper. They use tactile feedback to learn the properties of the deformable parts, and thus determine the minimum force needed to lift the deformable part. Heinrich and Worn's edited collection of papers [Heinrich00] describes deformation models and control algorithms for the manipulation of deformable objects. These include the modeling of fabrics, continuous modeling of deformation of linear objects such as beams, collaborative manipulation of deformable parts, laying out wires and cables and sewing.

Hirai et al [Hirai01] propose a robust control law for the manipulation of deformable parts. They use tactile feedback from the actuators and video feedback for the positions of selected reference points to control the motion of a deformable part. Li et al [Li02] design fixtures for laser welding using a genetic algorithm within robust design spaces with low to part dimension and jaw location errors. Li et al [Li02b] describe a dexterous part holding mechanism based on vacuum cups and model the elastic deformation of the sheet-metal part using Finite Element Methods and a statistical data model. The results from this model are used to minimize the part's deformation. Shiu et al [Shiu97, Shiu03] give a heuristic algorithm to analyze the deformation of a sheet metal part by decoupling it into beams based on the part's features, and give an algorithm to allocate tolerances to each feature.

Path planning for elastically deformable parts has been studied using probabilistic roadmaps (PRM). Holleman, Kavraki and Warren [Holleman98] give a path planning algorithm for a flexible surface patch. They use a Bezier approximation and an approximate energy function to model deformation of the part. They present experimental results of paths planned for parts generated by a search graph using PRM. Guibas et al [Guibas99] improve on the PRM methods for path planning for a surface patch by studying the medial axis of the workspace. Minimum energy configurations of the part are then computed for positions along the axis and connected by quasi-static paths. Lamiroux et al [Lamiroux99] generate a path for a thin rectangular elastic metal plate represented by a Bezier when it is manipulated by constraining the positions and orientations of two opposite edges. Given the controlling constraints, the shape of the plate is computed by minimizing the potential energy due to the deformations. If there is a collision between the plate and an

obstacle, the configuration is discarded. Paths are generated using PRM on the configurations of the edges being controlled. Moll and Kavraki [Moll04] have extended this approach to systems such as surgical sutures and snake robots by computing configurations using constrained minimization of potential energy with the length of the curve fixed.

As noted in the introduction, the present paper extends [Gopalakrishnan04] with a new metric for two-point deformation grasps and an algorithm for computing the optimal jaw separation.

3 Deformation-Space and Deform Closure

3.1 Deformation-Space

In this section, we summarize the relevant definitions and theorems from [Gopalakrishnan04]. We consider a linearly elastic deformable polygonal part E possibly containing polygonal holes. E is discretized into a triangular FEM mesh M with linear interpolation. The stiffness matrix for E and an initial undeformed configuration q_0 of E are also specified.

We define a Deformation Space (D-Space) D of the part. Each of the n nodes in M has two translational degrees of freedom (DOF). The D-space (deformation space) of the mesh is the smooth manifold $D = \mathbf{R}^{2n}$, with each coordinate axis corresponding to one DOF of an FEM node. Any deformed translated or rotated shape of this part can be represented as a unique point in D-space. For any point q in D , we denote the corresponding configuration of the part by $E(q)$.

We define $D_T(q_0)$ as the set of all q that have the same topology as initial configuration q_0 .

We consider frictionless contacts between E and a set of finger bodies A_i . Given a finger body A_i , its corresponding D-obstacle DA_i is the set of all configurations q such that $E(q)$ intersects A_i .

We define $D_{free} = \left(\bigcup_{i=1..k} DA_i \right)^c \cap D_T$ as the set of all feasible configurations.

D_{free}^c is the complement of D_{free} .

3.2 Potential Energy in D-Space

The nodal displacement vector X is the vector of the displacements of all nodes from their initial positions in configuration q_0 , expressed in the global coordinate frame used to define the FEM model (M, K, X) . X can be considered as a special case of expressing q when each node's degrees of freedom are expressed relative to a reference frame whose origin coincides

with the mesh node at configuration q_0 , and whose axes parallel to the axes of the global coordinate frame. For linear FEM with a stiffness matrix K , the potential energy at configuration q in D_{free} is given by:

$$U(q) = (1/2) X^T K X.$$

3.3 Deform Closure

We consider a configuration q_A in which the part is held by A .

Definition: An *equilibrium configuration* is any configuration at a local minimum of the potential energy in D_{free} . In the absence of friction and inertial forces, the part comes to rest at an equilibrium configuration.

Definition: We consider a set of wrenches that act on $E(q_A)$ for any equilibrium configuration q_A . If after the wrenches are applied and then removed, the part may not return to q_A , the wrenches are said to *release* E .

Definition: If $E(q_A)$ is held by A such that no sequence of wrenches that increases the deformation potential energy of E by at most U can release E from A , we say q_A satisfies the property *stable* (U).

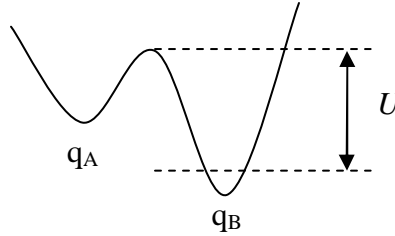


Fig. 2. A slice of the Potential Energy surface. q_A and q_B are stable equilibria. But for the shown value of U , only q_B satisfies stable (U).

Definition: The *threshold potential energy* U_A for A holding E in configuration q_A is defined as 1) $U_A(q_A) = \sup \{ U \mid q_A \text{ satisfies stable } (U) \}$ if q_A is an equilibrium configuration, and 2) 0 otherwise.

Definition: A holds $E(q_A)$ in *deform closure* if $U_A(q_A) > 0$.

Definition: A configuration with potential energy $U(q_A) + U_A(q_A)$ that E assumes when a sequence of wrenches releases it is called an *escape configuration*.

Given a rigid part, we call an undeformed deformable part with the same shape and configuration of the rigid part its equivalent deformable part.

We also prove the following theorems in [Gopalakrishnan04]:

Theorem 1: If A holds a rigid part in form closure, A will hold the equivalent deformable part in deform closure.

Theorem 2: Frame Invariance.

The definition of deform closure is frame invariant, i.e. it does not depend on the global reference frame used.

In the proof of theorem 2, we also show that the potential energy is frame-invariant.

4 Two-Point Deform-Closure Grasps: Optimal Jaw Separation

4.1 Quality Metric

As in the previous section, we consider the same deformable part model. Here, we consider two-point grasps, where there are exactly two contacting jaws (finger bodies). The initial placement of these jaws is specified as two mesh nodes n_0 and n_1 . The jaw separation, σ , is the Euclidean distance between the jaw contact points. In what follows, we describe our approach in terms of contracting grasps (where the contacts exert forces towards each other). An analogous approach can be developed for expanding grasps.

We define a quality metric Q to evaluate deform-closure grasps. We define σ^* as the jaw separation for which $Q(\sigma^*) = \max \{ Q(\sigma) \}$. Note that U_A , the threshold potential energy, is not an appropriate quality metric because to maximize it we would trivially close the jaws to the point where there is zero distance between them.

We introduce the elastic limit of part material to define a metric that balances the gripping force against forces that will result in plastic deformation of the part. Given the elastic limit strain e of the part material, we consider the maximum separation σ_L at which at least one mesh node reaches the elastic limit when squeezed by the contacts at n_0 and n_1 . We define $U_L(\sigma)$ as the difference between the potential energies at separations σ and σ_L . We define:

$$Q(\sigma) = \min \{ U_A(\sigma), U_L(\sigma) \}$$

At the optimal jaw separation σ^* , the potential energy needed to release the part equals the potential energy that would be required to squeeze it to its elastic limit.

4.2 Problem Description

Given linearly elastic polygonal part E , triangular mesh M , stiffness matrix K , initial undeformed configuration q_0 of E , elastic limit strain e_L , and a pair of mesh nodes n_0 and n_1 where a part is held by two frictionless point contacts, we give an algorithm that numerically determines contact separation σ_ε as an approximation to σ^* . The maximum allowed error in $Q(\sigma_\varepsilon)$ is specified as ε .

Input: Polygonal part E , mesh M with n mesh nodes and p perimeter nodes, stiffness matrix K , initial undeformed configuration q_0 , initial contact mesh nodes n_0 and n_1 , and parameters e_L and ε .

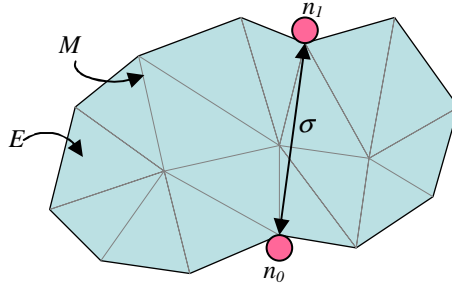


Fig. 3. Part E , mesh M , mesh nodes of contact (n_0, n_1) and stiffness matrix K are given as input to the algorithm. The algorithm numerically maximizes quality metric $Q(\sigma)$ where σ is the contact separation.

Output: A value of σ_ε such that $Q(\sigma_\varepsilon) \geq Q(\sigma^*) - \varepsilon$.

We make the following assumptions:

1. The perimeter of the part does not collide with itself intermediate configurations as it deforms from the deform-closure grasp to the escape configuration.
2. Mesh triangles do not become degenerate. In FEM practice, when mesh triangles become degenerate, a new, denser mesh is automatically generated. We assume that a sufficiently dense mesh that does not result in degeneracy is given initially.
3. If one contact is placed on the perimeter and the other is moved along the perimeter at a fixed separation from the first contact, the local maxima and minima of potential energy occur when the second contact is at a mesh node. Strictly speaking, given a particular mesh, the actual potential energy may be a maximum or a minimum even the contact is at an edge of the mesh, with the line joining the contacts being perpendicular to the edge. However, given a sufficiently dense mesh (with more mesh nodes near the contact), the difference between the maximum potential energy and the potential energy with the second contact at a vertex will be less than the error in potential energy predicted due to the FEM approximation of the part.

Our approach to solve this problem is detailed in the following sections. In brief, we make use of assumption 3 above to identify paths of interest in D-Space through which the part may be release from the grasp. We need not study all paths that release the part as long as we study one where the peak potential energy is at a minimum. Thus, due to assumption 3, we need only consider the paths where at least one contact is at a mesh node at any time. Among these paths, we focus on the points where both contacts are at mesh

nodes, since the potential energy varies monotonically between these points. This is a set of discrete configurations that we are interested in. We create a "contact graph" whose vertices these configurations and describe all paths of interest in D-Space as paths (traversal of edges) in this contact graph. This is done by constructing edges between graph vertices that differ in exactly one contact's position by exactly one mesh edge as the part slides out of the grasp. We add more edges for cases where the part need not slide out, but can move without contact with a jaw while maintaining a constant potential energy.

4.3 Constructing the Contact Graph

To compute σ_e , we would like to determine a path that the part can follow to be released with minimal increase in potential energy. Since it is inefficient to consider every possible path in D-space, we create a graph to represent key configurations as graph vertices.

We use the following notation: q_A is the initial configuration of the part when grasped by two contacts at $(0, 0)$ and $(\sigma, 0)$ engaging the part at n_0 and n_1 respectively. $\sigma(n_a, n_b)$ is the distance between mesh nodes n_a and n_b . $\sigma_0(n_a, n_b)$ is the distance between mesh nodes n_a and n_b at configuration q_0 .

To release the part from A , we move it along a path in D-space starting at q_A and ending at an escape configuration. To determine the threshold potential energy, we are interested in an escape configuration with least potential energy. From assumption 3, if one contact were fixed on the part's perimeter and the other jaw is allowed to slide along the perimeter, the potential energy as a function of the position of the second jaw is monotonic (increasing or decreasing) in every interval corresponding to one mesh edge. This implies: 1) there exists such an escape configuration q_p with both contacts at mesh nodes, and 2) there exists a path in D-space from q_A to q_p such that one of the contacts is always at an FEM node such that q_p has the maximum potential energy among all configurations on the path. It is sufficient to consider the paths where one contact is always at a mesh perimeter node.

We construct a "contact graph" G to represent such paths. The set of vertices in G is V . Each graph vertex in V represents a configuration as the part is released from the point contacts. Thus, every graph vertex $v(n_a, n_b)$ corresponds to point contacts present at a pair of perimeter mesh nodes n_a and n_b . Vertices $v(n_a, n_b)$ and $v(n_a, n_c)$ are connected by an edge if: 1) n_a and n_b are connected by a mesh edge on the part's perimeter, or 2) an arc centered on n_a and having radius σ and lying on the exterior of the part has one end point n_b and the other end-point on a mesh edge flanking n_c . The second case is when the part can be rotated about a mesh node till the contact reaches the perimeter near another mesh node.

4.4 Potential Energies at Graph Vertices

At each graph vertex, we are interested in the minimum possible potential energy when the contacts engage the part at the corresponding mesh nodes n_a and n_b , with separation σ . This is determined by solving the FEM model with boundary conditions restricting n_a at $(0, 0)$ and n_b at $(\sigma, 0)$.

We note that we use a linear FEM system to model the part. Hence, nodal deformations are computed by solving a system of linear equations subject to the boundary conditions. As a result, for any graph vertex when the two contacts perform a contracting grasp at (n_a, n_b) , the potential energy associated with the corresponding vertex is a quadratic function of σ given by $U(n_a, n_b, \sigma) = \frac{1}{2} k_{ab} (\sigma - \sigma_0(n_a, n_b))^2$, where k_{ab} is the x component of the force applied by the contacts towards each other when $\sigma_0(n_a, n_b) - \sigma = 1$ unit. However, for $\sigma > \sigma_0(n_a, n_b)$, the potential energy for contracting grasps is 0.

We first compute the value of k_{ab} for all $v(n_a, n_b)$ by solving the FEM model with boundary conditions n_a is at $(0, 0)$ and n_b is at $(\sigma_0(n_a, n_b) - 1, 0)$.

For the graph vertex $v(n_0, n_1)$ alone, we also compute the strains at each mesh node. We find the maximum strain over all nodes as e_{max} .

Thus each graph vertex $v(n_a, n_b)$ is associated with a potential energy $U(n_a, n_b, \sigma) = \frac{1}{2} k_{ab} (\sigma - \sigma_0(n_a, n_b))^2$, where k_{ab} are known. Some of these vertices correspond to equilibrium configurations. A vertex $v(n_a, n_b)$ is in equilibrium if for every neighbor $v(n_c, n_d)$ of $v(n_a, n_b)$,

$$U(n_c, n_d, \sigma) \geq U(n_a, n_b, \sigma).$$

4.5 Computing σ_ϵ

Consider a path from $v(n_a, n_b)$ to an equilibrium vertex. The path is a sequence of vertices. Each graph vertex $v(n_c, n_d)$ on the path has a potential energy function $U(n_c, n_d, \sigma)$. The potential energy needed to release the part through this path is given by the upper envelope of all these potential energy functions. There are many equilibrium nodes, and many paths to each equilibrium node. Each path has an upper envelope that gives the potential energy needed. If we consider all the upper envelopes over all the paths and take their lower envelope, this gives the minimum potential energy needed to release the part as a function of contact separation. The difference between this lower envelope and function $U(n_0, n_1, \sigma)$ is the threshold potential energy $U_A(\sigma)$ of the deform-closure grasp.

Recall from the previous section that we computed e_{max} , the maximum strain for a unit reduction of jaw separation from the undeformed configuration with the contacts at n_0 and n_1 . We use this to determine σ_ϵ as $\sigma_0(n_0, n_1) - (\epsilon / e_{max})$. The additional potential energy needed for the contacts to

squeeze the part to the elastic limit is given by $U_L(\sigma) = \frac{1}{2} k_{01} (\sigma_L^2 - \sigma^2)$. The quality metric is given by $Q(\sigma) = \min \{ U_A(\sigma), U_L(\sigma) \}$.

$Q(\sigma)$ is a continuous, piecewise differentiable function. However, the number of pieces may be exponential in the number of graph vertices. Hence, computing the exact function and maximizing the metric would require exponential time. Instead, we numerically sample the interval $[0, \sigma_0(n_0, n_1)]$ to maximize $Q(\sigma)$. We define $\lambda = \max \{ k_{ab} \sigma_0(a, b) \}$. With uniform sampling at intervals of size $\xi = \varepsilon / \lambda$, it can be shown that the error in the optimal metric is at most ε .

For all $\sigma_i = i \varepsilon / \lambda$, $i = 0, \dots, \lceil (\sigma_0(n_0, n_1) \lambda / \varepsilon) \rceil$, we find the threshold potential energy using the algorithm described below.

4.6 Computing Threshold Potential Energy

We are given a value σ_i of contact separation. As in the previous section, consider a path from $v(n_0, n_1)$ to equilibrium configuration $v(n_a, n_b)$. Let U_{max} be the maximum potential energy over all nodes traversed by this path. There are many equilibrium vertices and many such paths. Let U_p be the minimum of the U_{max} values over all such paths. The threshold potential energy $U_A(\sigma_i)$ is given by $U_p - U(n_0, n_1, \sigma_i)$.

We determine $U_A(\sigma_i)$ using the contact graph G by an algorithm inspired by Dijkstra's shortest path algorithm. We maintain a set Ω of vertices for whom we know minimum work needed to get to, and a list U_{min} of these minimum works. We also compute a list Ψ of estimated minima of work needed to reach vertices in $V - \Omega$ that are adjacent to vertices in Ω . The estimate is made assuming that in the path used to reach the node, the previous node lies in Ω . We then update Ω by adding the graph vertex with minimum Ψ .

Sub-procedure $U_A(\sigma_i)$:

1. Initialize $\Omega \leftarrow \{ v(n_0, n_1) \}$, $U_{min}(v(n_0, n_1)) = 0$, $\Psi(v(n_a, n_b)) = U(n_0, n_1, \sigma_i) - U(n_0, n_1, \sigma_i)$ for all vertices $v(n_a, n_b)$ adjacent to $v(n_0, n_1)$, $\Psi(v(n_a, n_b)) = \infty$ for others.
2. While $\Omega \neq V$
3. Do $v(n_c, n_d) \leftarrow \arg_min \{ \Psi(v(n_a, n_b)) \}$
4. $\Omega \leftarrow \Omega \cup \{ v(n_c, n_d) \}$
5. $U_{min}(v(n_c, n_d)) = \Psi(v(n_c, n_d))$
6. If $v(n_c, n_d)$ is an equilibrium vertex, return $U_{min}(v(n_c, n_d))$ and stop.
7. For each $v(n_a, n_b)$ in $V - \Omega$ adjacent to $v(n_c, n_d)$, update $\Psi(v(n_a, n_b)) \leftarrow \min \{ \max \{ \Psi(v(n_c, n_d)), U(n_a, n_b, \sigma_i) - U(n_0, n_1, \sigma_i) \}, \Psi(v(n_a, n_b)) \}$

We can prove that U_{min} always contains the minimum increase in potential needed to reach any element in Ω as follows: Initially, when $\Omega = \{v(n_o, n_l)\}$, this is true. When a vertex $v(n_c, n_d)$ is added to Ω , assume that U_{min} is larger than the minimum work needed to reach $v(n_c, n_d)$. This implies that in the path that needs to be taken to reach $v(n_c, n_d)$ to minimize the additional potential energy needed, the graph vertex preceding $v(n_c, n_d)$ is in $V - \Omega$. In the sequence of graph vertices represented by the path, consider the first graph vertex $v(n_a, n_b)$ in $V - \Omega$. $\Psi(v(n_a, n_b)) \geq \Psi(v(n_c, n_d))$. Thus, $U(v(n_c, n_d)) \geq \Psi(v(n_c, n_d))$. This is against the assumption that $U_{min}(v(n_c, n_d))$ is not the minimum possible.

4.7 Numerical Example

We consider a part shown in Figure 4. The part material is rubber with the standard Young's modulus of 2 MPa, and Poisson ratio of 0.1. The strain at the elastic limit was taken as 0.8. The undeformed distance between the mesh nodes shown is 10 mm. We modeled the part using I-deas and ANSYS and determined σ_e for the mesh shown. Each FEM problem was solved in about 0.28 seconds. The optimal contact separation is 5.6 mm.

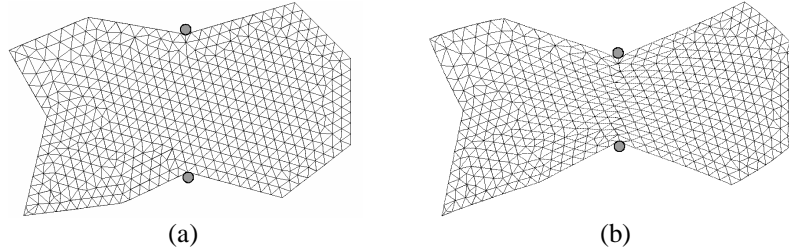


Fig. 4. (a) Example part with initial jaw separation 10mm for the perimeter mesh nodes shown. (b) The same part at optimal jaw separation at optimal jaw separation 5.6 mm.

5 Discussion

5.1 Complexity

As shown by [Ramamurti98], FEM systems can be solved exactly in $O(n^3)$ time for a part with n mesh nodes. For a part with n mesh nodes and p perimeter nodes, the graph used for the algorithm has $O(p^2)$ nodes and $O(p^2)$ edges. Thus, pre-computing the k_{ab} values for each graph vertex requires $O(n^3 p^2)$ time. Computing U_A for a known separation requires $O(p^2 \log p)$ time when the graph is implemented as a binary heap (this complexity is identical to that of Dijkstra's algorithm for sparse graphs). This iteration needs

to be performed $(\sigma_0(0, 1) \lambda / \epsilon)$ times for each grasp, sampling at points with distance ϵ/λ between them. Thus, σ_ϵ can be computed in $O(n^3 p^2 + p^2/\epsilon \log p)$ time.

5.2 Conclusion

We defined a new measure of grasp quality for two-point deform-closure grasps. This metric is based on balancing the potential energy needed to release the part against the potential energy that would result in plastic deformation. Given two jaw contacts at the perimeter nodes, we give a numerical algorithm to determine the optimal jaw separation based on this metric. For a part with n mesh nodes and p perimeter nodes, the algorithm computes an approximation to the optimal separation in time $O(n^3 p^2 + (p^2/\epsilon) \log p)$.

We are currently studying how U_A varies with increasing mesh density, and the minimal mesh needed to define deform-closure. We are also investigating the optimal choice of initial contact nodes and the accounting for friction in our algorithm.

Acknowledgements

We thank Frank van der Stappen, Rama Koganti, Matt Zaluzec, Ron Alterovitz, Dezheng Song and Vladlen Koltun and the anonymous reviewers for their valuable comments.

References

- [Bicchi00] A. Bicchi and Vijay Kumar, Robotic Grasping and Contact: A Review, Proceedings of IEEE International Conference on Robotics and Automation, pp348-353, 2000.
- [Brost96] R.C.Brost and K.Y.Goldberg, "A complete algorithm for designing planar fixtures using modular components," IEEE Trans. On Robotics and Automation, vol. 12, no. 1, pp. 31 – 46, 1996.
- [Cai96] Cai W., Hu S.J., Yuan J.X., Deformable sheet metal fixturing: principles, algorithms, and simulations. Transactions of the ASME. Journal of Manufacturing Science and Engineering, vol.118, (no.3), ASME, Aug. 1996. p.318-24.
- [Cheong02] Cheong, J.-S., Goldberg K., Overmars M.H. and van der Stappen, A.F., Fixturing Hinged Polygons, Proceedings, IEEE International Conference on Robotics and Automation, pp. 876-881, 2002.
- [Cheong03] Jae-Sook Cheong, Herman J. Haverkort, and A. Frank van der Stappen, On Computing All Immobilizing Grasps of a Simple Polygon with Few Contacts accepted for ISAAC (International Society for Analysis, its Applications and Computation), 2003.
- [Corman90] T.H. Corman., C.E. Leiserson. and R.L. Rivest, Introduction to Algorithm, MIT Press, 1990.
- [Doulgeri04] Doulgeri, Z. and Peltekis, J., Modeling and Dual Arm Manipulation of a Flexible Object, IEEE International Conference on Robotics and Automation, April 2004.

- [Gopalakrishnan02] K. "Gopal" Gopalakrishnan, Ken Goldberg, Gripping parts at concave vertices, IEEE International Conference on Robotics and Automation, 2002, Page(s): 1590 - 1596, Volume: 2, 2002.
- [Gopalakrishnan03] K. "Gopal" Gopalakrishnan, Matthew Zaluzec, Rama Koganti, Patricia Deneszcuk and Ken Goldberg, "Unilateral" Fixturing of Sheet Metal Parts Using Modular Jaws with Plane-Cone Contacts, Proceedings, IEEE International Conference on Robotics and Automation, pp 3953-3958, 2003.
- [Gopalakrishnan04] K. "Gopal" Gopalakrishnan and Ken Goldberg, D-Space and Deform Closure: A Framework for Holding Deformable Parts, IEEE International Conference on Robotics and Automation (ICRA), May 2004.
- [Guibas99]Guibas, L.J.; Holleman, C.; Kavraki, L.E.; A probabilistic roadmap planner for flexible objects with a workspace medial-axis-based sampling approach, Intelligent Robots and Systems, 1999. IROS '99. Proceedings. 1999 IEEE/RSJ International Conference on, Volume: 1, 17-21 Oct. 1999, Page(s): 254 -259 vol.1.
- [Heinrich00]Heinrich D. and Worn H., editors, Robot manipulation of deformable objects, Springer Verlag, May 2000.
- [Hirai01] Hirai S., Tsuboi T., Wada T., Robust Grasping Manipulation of Deformable Objects, Proc. IEEE Symposium on Assembly and Task Planning, pp.411-416, Fukuoka, May, 2001
- [Holleman98] Holleman, C.; Kavraki, L.E.; Warren, J., Planning paths for a flexible surface patch, Robotics and Automation, 1998. Proceedings. 1998 IEEE International Conference on, Volume: 1, 16-20 May 1998, Page(s): 21 -26 vol.1.
- [Howard97] Howard, A.M. and Bekey, G.A., Recursive Learning for Deformable Object Manipulation, 8th International Conference on Advanced Robotics, pp. 939-944, Monterey, CA, July 7-9, 1997.
- [Lamiriaux99] Lamiriaux, F.; Kavraki, L.E.; Path planning for elastic plates under manipulation constraints, Robotics and Automation, 1999. Proceedings. 1999 IEEE International Conference on, Volume: 1, 10-15 May 1999, Page(s): 151 -156 vol.1.
- [Li02] Li B., Shiu B.W., Lau K.J., Fixture configuration design for sheet metal assembly with laser welding: a case study. International Journal of Advanced Manufacturing Technology, vol.19, (no.7), Springer-Verlag, 2002, p.501-9.
- [Li02b] Li H. F., Ceglarek D., Shi J., A Dexterous Part-Holding Model for Handling Compliant Sheet Metal Parts, ASME Transactions, Journal of Manufacturing Science and Engineering. Vol. 124, No. 1, pp. 109-118, 2002.
- [Markenscoff90] X. Markenscoff, L. Ni and C. H. Papadimitriou, The Geometry of Grasping, International Journal of Robotics Research, Vol. 9, No. 1, pp 61-74, 1990.
- [Mason01]Mason M.T., Mechanics of Robotic Manipulation, The MIT Press, 2001.
- [Menassa91] Menassa R., De Vries W., Optimization Methods Applied to Selecting Support Positions in Fixture Design, ASME Journal of Engineering for Industry, vol 113, pp. 412-418, 1991.
- [Milgram02] Milgram, R.J. and Trinkle, J.C., "The Geometry of Configuration Spaces for Closed Chains in Two and Three Dimensions," Homology Homotopy and Applications, 2002.
- [Mishra87]B. Mishra, J. Schwarz, and M. Sharir, On the existence and Synthesis of Multifinger Positive Grips, Algorithmica 2, 1987.
- [Moll04] Moll, M. and Kavraki L., Path Planning for Minimal Energy Curves of Constant Length, Proceedings, IEEE International Conference on Robotics and Automation, 2004.
- [Ramamurti98] Ramamurti V., Computer Aided Mechanical Design and Analysis, McGraw Hill Book Company, July 1998.
- [Reuleaux1876] F. Reuleaux, The Kinematics of Machinery. New York: Macmillan 1876, republished by New York: Dover, 1963.
- [Rimon96]Rimon E. and Burdick J., On force and form closure for multiple finger grasps, Proceedings of IEEE International Conference on Robotics and Automation, 1996, pp. 1795 -1800 vol.2.
- [Rimon98]Elon Rimon and Joel Burdick, Mobility of bodies in contact - I, IEEE transactions on Robotics and Automation, 14(5): 696-708, 1998.

- [Rimon99] Rimon, E. and Blake, A., Caging planar bodies by one-parameter two fingered gripping systems, *International Journal of Robotics Research*, v18, n3, March 1999, pp. 299-318.
- [Rong99] Rong, Y. and Zhu, Y., "Computer-aided Fixture Design", Marcel Dekker, ISBN: 0-8247-9961-5, New York, 1999.
- [Selig00] J. M. Selig. *Geometrical Foundations of Robotics*. World Scientific, 2000.
- [Shiu97] Shiu, B.W., Ceglarek, D., Shi, J., 1997 "Flexible Beam-Based Modeling of Sheet Metal Assembly for Dimensional Control," *Trans. of NAMRI*, Vol. XXV, pp. 49-54.
- [Shiu03] Shiu, B.W., Apley, D., Ceglarek, D., Shi, J., 2003 "Tolerance Allocation for Sheet Metal Assembly using Beam-Based Model", *Trans. of IIE, Design and Manufacturing*, Vol. 35, No. 4, pp. 329-342. (April 2003). The paper was also summarized and featured in the March 2003 edition of *Industrial Engineer* (formerly *IIE Solutions*).
- [Somoff1900] P. Somoff, *Über gebiete von schraubengeschwindigkeiten eines starren körpers bievverschiedener zahl von stuz achen*, *Zeitschrift für Mathematic and Physik*, vol. 45, pp. 245-306, 1900.
- [vanderStappen99] Van der Stappen A.F., Wentink C., Overmars M.H., Computing form-closure configurations, *Proceedings of IEEE International Conference on Robotics and Automation*, vol.3, pp. 1837 -1842, 1999.
- [Wakamatsu96] Wakamatsu, H., Hirai, S., and Iwata, K., Static Analysis of Deformable Object Grasping Based on Bounded Force Closure, *Proc. IEEE Int. Conf. on Robotics and Automation*, Vol.4, pp.3324-3329, Minneapolis, April, 1996.
- [Zhu03] Zhu X., Ding H., Wang J., Grasp analysis and synthesis based on a new quantitative measure, *IEEE Transactions on Robotics and Automation*, vol. 19, no. 6, pp. 942-953, Dec. 2003.